

# Probability analysis of optimal design for fatigue crack of aluminium plate repaired with bonded composite patch

H. Errouane<sup>1</sup>, N. Deghoul<sup>1</sup>, Z. Sereir<sup>\*1</sup> and A. Chateauneuf<sup>2</sup>

<sup>1</sup>Laboratoire Structures de Composites et Matériaux innovants, Faculté de Génie Mécanique, Université des Sciences et de la Technologie d'Oran, BP 1505 El M'naouer, USTMB, Oran, Algérie

<sup>2</sup>Clermont Université, Blaise Pascal, EA 3867, LaMI, BP 10448, 63000 Clermont-Ferrand, France

(Received April 8, 2016, Revised October 6, 2016, Accepted October 19, 2016)

**Abstract.** In the present study, a numerical model for probability analysis of optimal design of fatigue non-uniform crack growth behaviour of a cracked aluminium 2024 T3 plate repaired with a bonded composite patch is investigated. The proposed 3D numerical model has advanced in literatures, which gathers in a unique study: problems of reliability, optimization, fatigue, cracks and repair of plates subjected to tensile loadings. To achieve this aim, a finite element modelling is carried out to determine the evolution of the stress intensity factor at the crack tip Paris law is used to predict the fatigue life for a given crack. To have an optimal volume of our patch satisfied the practical fatigue life, a procedure of optimization is proposed. Finally, the probabilistic analysis is performed in order to show that optimized patch design is influenced by uncertainties related to mechanical and geometrical properties during the manufacturing process.

**Keywords:** composites; fatigue; optimizations; numerical methods; structural reliability; simulation, fracture mechanics

## 1. Introduction

Now days, many industrial sectors are facing the challenge of aging structures in their inventories. These structures aging are mainly due to damage from fatigue cracking and corrosion. Therefore, repair with dependable techniques to restore the structural integrity becomes mandatory. The concept of using bonded composite materials is powerful a mean to maintain cracked metallic structures in acceptable service conditions. Technically, bonded repair reduces the stress field near the crack by bridging the stresses between the cracked plate and the composite patch, leading to retardation or complete stopping of the crack growth. The technique provides a high structural efficiency and extends the lifetime of cracked structural components with economic cost (Baker *et al.* 2002, Wang *et al.* 2014).

The investigation of crack growth behaviour of bonded patch repaired structures has been studied by many authors. Denney and Mall (1997) conducted a series of experiments to investigate the effects of disbond location and size on the fatigue response of cracked thin aluminium panels repaired with bonded composite patches. A disbond around the crack results in larger crack growth rate and shorter life compared to a disbond away from the crack and a completely bonded patch. A combined boundary element method and finite element method employed by (Sekine *et al.* 2005) to investigate the fatigue crack growth behaviour of cracked

aluminium panels repaired with an adhesively bonded fiber-reinforced polymer (FRP) composite patch. Numerical simulation of crack growth process of a cracked aluminium panel repaired with a FRP composite patch under uniaxial cyclic loading has been carried out. So and Lee (2002) investigated the fatigue crack growth behaviour of thick panel repaired with bonded composite patch using the stress intensity factor range and fatigue crack growth rate. In this study two types of crack front modelling, i.e. uniform crack front model and skew crack front model, were used. The stress intensity factor calculated using FEM was compared with the experimentally determined values and provides good results.

Interesting experimental and numerical works were presented by (Hosseini-Toudeshky *et al.* 2007, 2009) in order to investigate the fatigue crack growth life and crack propagation in repaired thin and thick aluminum panels under mode-I, mixed mode and thermal conditions. These authors showed that the maximum difference between the lifetimes obtained from the non-uniform crack growth modeling and the experimental results are about 10% in Mode-I. However, in mixed mode, the most fatigue crack growth life extension belongs to the repaired panel with the patch lay-up of [90]<sub>4</sub>. It was also shown that the predicted crack growth lifetime using the unpatched surface models is too conservative and it may be 50% non-conservative when the mid-plane results are used. The experimental results showed that, the crack propagation life of the panels may increase by the order of 30-85% depending on the used patch lay-up. Fracture analysis and remaining life prediction for aluminum alloy (Al2014A) plate panels with concentric stiffener by varying sizes and positions under fatigue loading has been carried out by Ramachandra Murthy (2015). Domain integral technique has been used to

\*Corresponding author, Professor  
E-mail: serzou@hotmail.com

compute the Stress intensity factor (SIF) for various cases. They concluded that the remaining life for stiffened panel for particular size and position can be estimated by knowing the remaining life of corresponding un-stiffened panel. More recently, the fatigue durability of aluminum alloy 7075-T6 bonded joints representing aircraft structure repairs with and without the presence of a clad layer, was investigated by Harman and Rider (2013). The analysis showed that the cracking caused a substrate stress concentration which may have caused the clad fracture. Further analysis, supported by test observations, showed that once a small notch has been formed at the interface, the damage progression through the outer strap becomes.

Nevertheless, patch repairs must assure a given level of efficiency and bond durability under service conditions, since badly repaired structures can behave worse than the corresponding unrepaired ones Tsai and Shen (2004). For such a reason, the design of efficient patch repairs is a crucial task, which is very important from both economic and technical points of view. The choice of an optimal shape could be a good way to obtain the desired performance, in order to get the maximum structural safety to cost ratio. In this way, Brighenti (2007) determined the optimal shape of a patch repair for a cracked plate under both Mode I or Mode II fracture types by applying the Genetic Algorithms (GA). The best patch topology is obtained by finding the optimal patch material density distribution in an allowable given domain in which the repair is assumed to remain confined. The Genetic Algorithm is developed here to find out the extreme values of appropriate objective functions: the optimal patch shape minimizing the stress intensity factor or maximizes the number of allowable cycles. More recently, (Errouane *et al.* 2014) proposed a 3D numerical model for the optimization of composite patch repair of an aluminum 2024 T3 plate containing a central crack. To achieve this aim, a finite element modelling is carried out to determine the evolution of the stress intensity factor at crack tip. The crack length has been varied to investigate the patch performance. To have an optimal volume of the patch satisfying the stress intensity factor, two methods of optimization called the sub-problem approximation method and the first order method were applied. From the results, the volume of the patch can be reduced until 57% and the stacking sequence  $[90^{\circ}4]$  gives a considerable reduction of the stress intensity factor.

However, simulation-based multidisciplinary optimization generates deterministic optimum design, which is frequently pushed to the limits of design constraint boundaries, leaving little or no room for uncertainty in modeling, simulation uncertainties, and manufacturing imperfections. Consequently, deterministic optimum designs that are obtained without consideration of uncertainty may result in unreliable designs, indicating the need for Reliability-Based Design Optimization (Youn *et al.* 2004). In order to ensure that the bonded patch repaired structures are reliable and safe in case of cyclic loading, it is very important to evaluate uncertainties associated with loads, material properties, geometrical parameters, boundaries and other parameters (Padula *et al.* 2006).

In this framework, the present paper develops a probability analysis of optimal design approach for

modeling the fatigue crack growth behavior of cracked aluminum panels repaired with an adhesively bonded FRP patch. The proposed 3D numerical model gather in a unique study: problems of reliability, optimization, fatigue, cracks and repair of plates subjected to tensile loadings. Firstly, a 3D finite element model is developed in order to compute the stress intensity factor for repaired cracks with bonded composite patch. Secondly, first order method is applied to determine the optimal volume of the patch as well as adhesive thickness. The design criteria are related to the admissible stress intensity factor at the crack tip. Finally, a probabilistic model is developed in order to study the sensitivity of initial and optimized patch dimensions under cyclic loading. For this purpose, Monte Carlo Simulation (MCS) method is used to study the initial estimates and sensitivity of the response variables regarding geometrical and mechanical properties of adhesive layer, aluminum and FRP plates.

## 2. Computational fatigue and fracture analysis

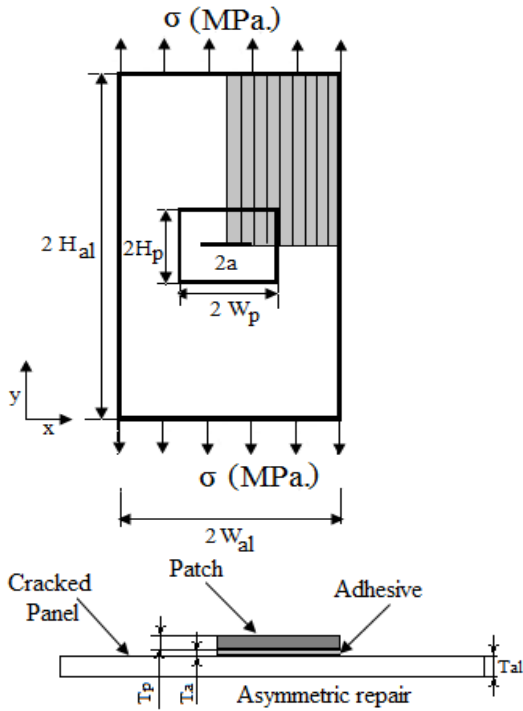
To assess the fatigue life, a 3D finite element analysis is carried out for crack growth of single-side repaired aluminum plate under uniaxial loading. The fatigue crack growth in aluminum panel repaired with a rectangular FRP composite patch, shown in Fig. 1. The dimensions and material of the cracked panel (2024-T3 aluminum) are the same of those given by Housseini (2007). Class/epoxy unidirectional lay-up perpendicular to the crack length is used for the patch. The dimensions of the cracked aluminum panel, FRP composite patch and adhesive layer are determine in Fig.1, and the corresponding mechanical properties are shown in Table 1. The cracked aluminum panel is subject to cyclic stress with maximum stress  $\sigma_{\max}=118$  MPa and the stress ratio  $R=0.05$ . The initial crack length on the surface of this cracked panel repaired with composite patch is  $2a=10$  mm, which is propagated until 28 mm.

The 3D numerical model used in these investigations is carried out using Ansys as shown in Fig. 2(a). 20-node isotropic brick elements (Solid 95) were used for Aluminum plate and adhesive. But for the patch, anisotropic brick elements (Solid 46) are chosen to model the properties of each layer of the laminated plate. The adhesive layer was meshed with one layer of finite elements and the composite patch with four layers. Because of singularity, only quarter-point crack-tip elements were used to model the crack tip region. The mesh density was increased in the region in which the crack is more likely to evolve as depicted in Fig. 2(b).

In order to assess the lifetime of the repaired structure, the fatigue crack growth rate is needed.  $da/N$ , which can be computed by Paris law (Lee and Lee 2004)

$$\frac{da}{dN} = C \Delta K^m \quad (1)$$

where  $m$  and  $C$  are material constants, given by  $3.2828$  and  $3.63 \cdot 10^{-13}$  respectively for thin panels and  $4.224$  and  $1.51 \cdot 10^{-15}$  for thick panels (Housseini-Toudeshky *et al.*



Length of plate	$H_{al}$	= 50 mm
Width of plate	$W_{al}$	= 25 mm
Thickness of plate	$T_{al}$	= 2.29 mm
Length of patch	$H_p$	= 20 mm
Width of patch	$W_p$	= 17.5 mm
Thickness of patch	$T_p$	= 0.72 mm
Thickness of adhesive	$T_a$	= 0.1 mm
Length of crack	$a$	= 5 to 14 mm

Fig. 1 Typical geometry and loading of single-side repaired panels (Hosseini-Toudeshky *et al.* 2007)

Table 2 Material properties of the panel, adhesive layer and patch (Hosseini-Toudeshky *et al.* 2007)

Material	$E_1$ (GPa)	$E_2, E_3$ (GPa)	$\nu_{12}, \nu_{13}$	$\nu_{23}$	$G_{12}, G_{13}$ (GPa)	$G_{23}$ (GPa)
Aluminium 2024T3	71.3	/	0.33	/	/	/
Glass/Epoxy	50	14.5	0.33	0.33	2.56	2.24
Adhésif	1.89	/	0.33	0.33	/	/

2007),  $\Delta K$  is the stress intensity factor range in fatigue loading,  $N$  is the number of cycles, and  $da$  is the crack increment. The stress intensity factor range is normalized using the following formula:

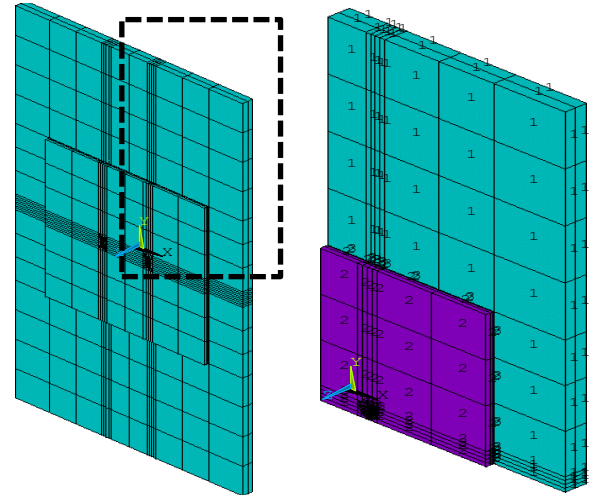
$$\Delta\sigma = \sigma_{\max} - \sigma_{\min} = \sigma_{\max} (1 - R)$$

where  $\Delta\sigma$  is, the stress range

A common approach for estimating fatigue life is to integrate the Paris equation to give

$$N_f = \int_{a_0}^{a_f} \frac{1}{C(\Delta K_I)^m} da \quad (2)$$

where  $N_f$  is the number of cycles required for the initial crack,  $a_0$ , to grow to the size  $a_f$ .



(a) Complet model (b) Quarter portion  
Fig. 2 Typical finite element mesh of single-side repaired panel

Since  $\Delta K$  varies with the crack length, Euler algorithm is often used

$$N^{(j+1)} = N^{(j)} + \Delta N^{(j)} = N^{(j)} + \frac{\Delta a^{(j)}}{C[\Delta K(a^{(j)})]^m} \quad (3)$$

with  $j=0, 1, 2, \dots, n$

where  $n$  is the total number of increments.

In many studies on fatigue life assessment for single-sided repairs, the crack front in every step is pre-assumed to be a uniform. From the fact that Stress Intensity Factor SIF varies along the crack front requires some averaging method, named global increment of crack growth (Fig. 3). Moreover, if the local increments along the crack front are considered as shown in Fig. 4, Paris law can be used at any point along the crack front as

$$\frac{da_i}{dN} = C(\Delta K_i)^m \quad (4)$$

to relate  $da_i$  to  $\Delta K_i$  which are respectively the local normal

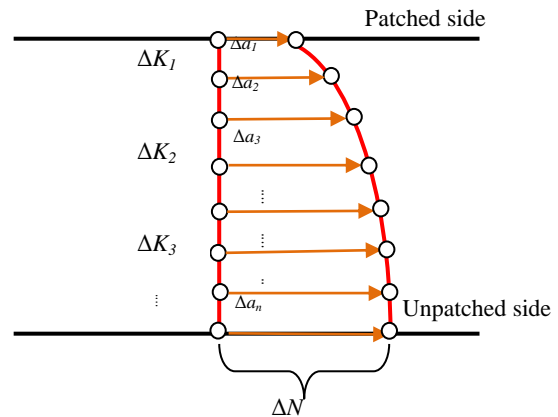


Fig. 3 Local increment of crack growth (Youn *et al.* 2004)

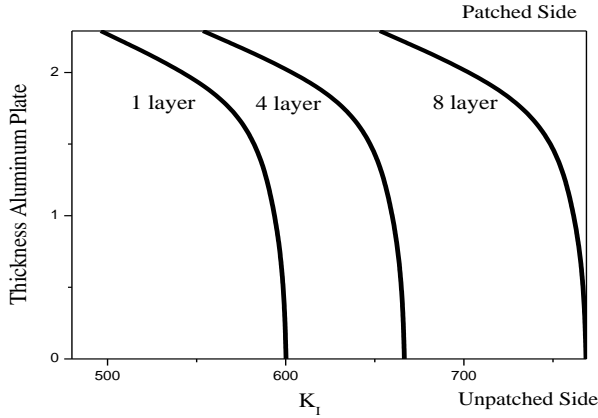


Fig. 4 Predicted  $K_I$  for the local increment

crack growth increment and stress intensity factor range at an arbitrary point  $i$  along the crack front as shown in Figs. 3-4. Similarly, the following equation can be derived

$$\Delta a_i^{(j)} = \left( \frac{\Delta K_i^{(j)}}{\Delta K_{\max}^{(j)}} \right)^m \Delta a_{\max}^{(j)}, \quad i = 1, 2, \dots \quad (5)$$

$$\Delta N^{(j)} = \frac{\Delta a_{\max}^{(j)}}{C \left( \Delta K_{\max}^{(j)} \right)^m} \quad (6)$$

where  $\Delta a_{\max}^{(j)}$  is the maximum crack growth increment at the point where the maximum stress intensity factor range,  $\Delta K_{\max}^{(j)}$ , along the crack front occurs.

### 3. Fatigue crack growth life

In order to check the precision of the developed numerical model, the obtained fatigue crack growth life of the repaired thick panels using FEM are compared with experimental results performed by (Hosseini *et al.* 2007) with and without bonded patch. Fig. 5 represents, the variation of crack length versus the number of load cycles for both unrepaired and repaired panels with four layers of glass/epoxy patch for thin aluminum plate ( $T_{al}=2.29$  mm).

The good agreement between our model and results in literature (Hosseini *et al.* 2007) validates the developed FEM non-uniform crack growth procedure for patched and unpatched cracked aluminum plate as well as the material constants used for the Paris law.

It is noticed from this figure that composite patch repair can significantly improve the fatigue life of the substrate. At the final crack length ( $a=14$  mm), the number of cycles increases from 21479 for unpatched plate to 34479 for 4-layer patched plate (almost 38%).

In order to quantify the fatigue crack growth life, the number of cycles at final crack length ( $a=14$  mm) is given in table 2 for our model, compared with experimental results given in (Harman *et al.* 2013). Comparatively to experimental and numerical models of Hosseini (2007), our 3D numerical model is very accurate because it uses the local increment load (Fig. 4) in which the stress intensity

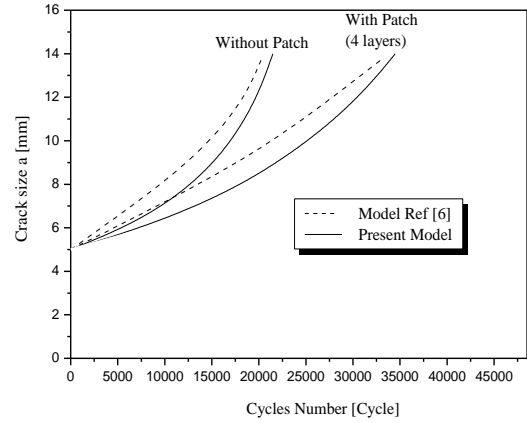


Fig. 5 Crack length versus the number of cycles for repaired and unrepaired thin aluminum plate

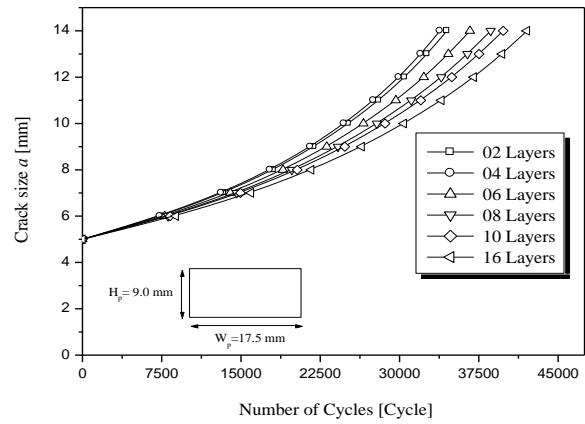


Fig. 6 Crack size variation versus the number of cycles for a height of patch  $H_p=9.0$  mm

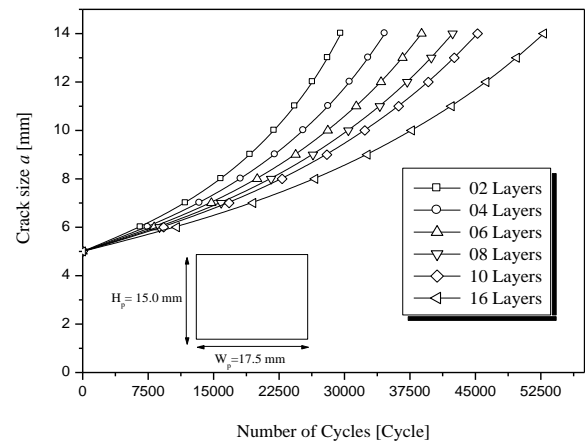


Fig. 7 Crack size variation versus the number of cycles for a height of patch  $H_p=15.0$  mm

factor varies along the thickness of the cracked plate. Figs. 6 and 7 are plotted in order to emphasize the patch geometrical variation on the fatigue non-uniform crack growth behaviour of the cracked aluminium 2024 T3 plate repaired with a bonded composite patch.

According to reference (Errouane *et al.* 2014), it was noted that the relationship between the height and the width

Table 3 Volume of the patch and fatigue crack growth life according to number of layers

Height of the patch	Volume/ Cycles	2 layers	4 layers	6 layers	8 layers	10 layers	16 layers
9 mm	Volume of patch	56.7	113.4	170.1	226.8	283.5	453.6
	Number of cycles	29681.6	33827	36662	38617	39808	42046
12 mm	Volume of patch	75.6	151.2	226.8	302.4	378	604.8
	Number of cycles	29688	34449	38163	41075	43189	48168
15 mm	Volume of patch	94.5	189	283.5	378	472.5	756
	Number of cycles	29591.5	34618	38830	42392	45241	52839

of the patch must be carefully selected in order to sufficiently cover the cracked zone, which will allow for good reduction of stress intensity factor.

From Fig. 6, it is clear that for low height of the patch  $H_p=9.0$  mm, the number of cycles is rather reduced. Moreover, there is no significant difference between the lives obtained for 2 layers to 10 layers' patches. On the other hand, when the height of the patch  $H_p=15.0$  mm (Fig. 7) becomes significant, the lifespan becomes more appreciable, especially when increasing the number of patch layers. In addition, the patch tends to have a square form for which the stress intensity factor is minimal, succeeding front size a large life extension. A qualitative and quantitative comparison was presented in Table 3 to emphasize the effect of patch geometry on fatigue crack growth life of the aluminum plate.

#### 4. Fatigue life optimization

The various optimization methods proposed in the literature (Mahadesh Kumar and Hakeem 2000, Yan 2004) enable us to find the optimal structure shape with low cost and suitable service conditions. The concept of shape optimization is based on the formulation and parametric modeling of the objective function, which can be the weight, the volume, the stress, the cost, or any other factors. In the present model, the optimization technique is applied on the volume of composite patch repair of an aluminum 2024 T3 plate containing a central crack. The proposed optimization procedure is implemented in Ansys FEM. The first order method converts the problem to an unconstrained one by adding penalty functions to the objective function. However, unlike the sub problem approximation method, the actual finite element representation is minimized and not an approximation. The first order method uses gradients of the dependent variables with respect to the design variables. For each iteration, gradient calculations (which may employ a steepest descent or conjugate direction method) are performed in order to determine a search direction, and a line search strategy is adopted to minimize the unconstrained problem. Thus, each iteration is composed of a number of sub-iterations that include search

direction and gradient computations. That is why one optimization iteration for the first order method performs several analysis loops.

The structural optimization reported in this work is performed on a composite patch volume use to repair an aluminum Plate 2024-T3 containing a central crack. The main objective is to find a minimal patch volume with satisfactory stress concentration at the crack tip of aluminum Plate. To achieve this aim three functions (design variables or parameters, an objective function) must be suitably defined.

To perform the optimization, the first step involves the definition of the design variable (DV); idealized geometrical characteristics of our patch (length, width and thickness) with an appropriate loads and boundary conditions. Secondly, the state variables (SV) are selected on the basis of the parametric study carried out in the previous section, where the performance of aluminum plate repair depends on the stress intensity factor at the crack tip  $K_I$  and on the interfacial shear stress  $\tau_{yz}$ . Finally, the objective function to be minimized is the amount of patch materials used for repair the volume of FRP plate. To minimize the patch volume for an aluminum plate 2024 T3 containing a central crack repaired by FRP plate, the mathematical formulation of the optimization problem is defined as follows

Minimize the objective function

$$V_p = f(H_p, W_p, T_p) \quad (7)$$

Subject to the constraints on the state variables

$$\begin{cases} K_I(H_p, W_p, T_p, H_C) \leq K_{IC} / \gamma \\ \tau_{yz} \leq 3.0MPa / \alpha \end{cases} \quad (8)$$

And the limits on the design variables

$$\begin{cases} \underline{W}_p \leq W_p \leq \bar{W}_p \\ \underline{H}_p \leq H_p \leq \bar{H}_p \\ \underline{T}_p \leq T_p \leq \bar{T}_p \end{cases} \quad (9)$$

where,  $V_p=H_p \times W_p \times T_p$  is the volume of the patch (FRP plate).

The under-bars ( $\underline{W}_p, \underline{H}_p, \underline{T}_p$ ) and over-bars ( $\bar{W}_p, \bar{H}_p, \bar{T}_p, \bar{g}_i$ ) represent the lower and upper bounds of the design variables respectively.  $\gamma$  and  $\alpha$  are the safety factors equal to 1.5 and 1.2 respectively.

In order to minimize the volume, it is necessary to respect the imposed state variable constraints.

These parameters are evaluated according to the upper and lower limits of the design variables ( $H_p, W_p, T_p$  and  $H_a$ ) given in Table 4 for the maximal tensile cyclic loading  $\sigma_{max}=118$  MPa and the stress ratio  $R=0.05$ .

The optimization is made only for the maximal crack ( $a=14$  mm) of aluminum repaired panel because it represents the most critical case.

By considering the aluminum 2024 T3 plate repaired with patch initial of volume  $V=252$  mm<sup>3</sup>, the optimization was accomplished to find an optimal patch shape in accordance with Fig. 8. Fig. 9 illustrates the iterations for

Table 4 Upper and lower limits of design and state variables

	Design variables						State variables	
	$W_p$ (mm)		$H_p$ (mm)		$T_p$ (mm)		$K_I$ (MPa $\sqrt{\text{mm}}$ )	
	min	max	Min	max	min	max	min	max
Case 1	7.0	15.0	5.0	15.0	0.1	0.25	650	$K_{IC}/1.5$
Case 2	<b>Fixed (17.5)</b>		5.0	15.0	0.1	0.25	650	$K_{IC}/1.5$
Case 3	7.0	15.0	5.0	15.0	<b>Fixed (0.18)</b>		650	$K_{IC}/1.5$

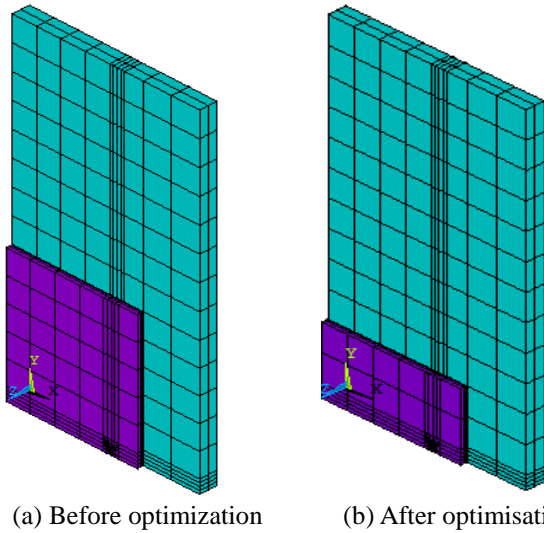


Fig. 8 Volume of the patch before and after optimization for half crack length of 14 mm

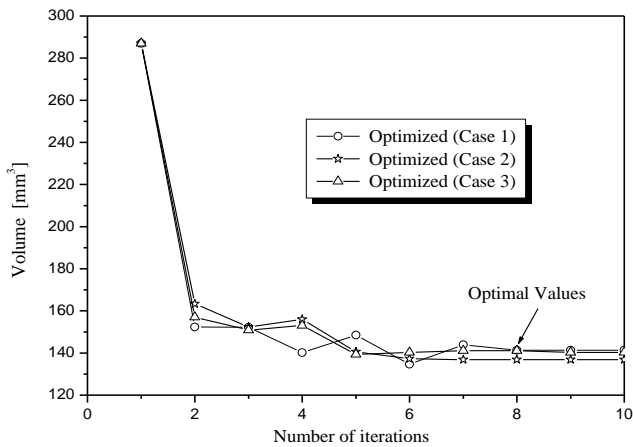


Fig. 9 Evolution of optimal patch for the three cases as function of the number of iterations

the patch volume optimization in the three cases given in Table 5.

From this figure, we can distinguish three zones: the first zone, up to iteration 2, in which convergence is still far and patch volume is high, the zone of random designs (located between the 3rd and 8th iterations), in which constraints are not fully satisfied, and finally the feasible zone in which a stable convergence is obtained leading to the optimal volume.

It is noted that the second case offers a better optimal volume 119 mm<sup>3</sup>, with approximately 53% of the initial volume.

Table 5 Optimal design variables and volume of the patch ( $a=14$  mm)

	Dimensions to be optimized	Values of optimized dimensions
Case 1	$H_p$ (mm)	10.32
	$W_p$ (mm)	17
	$T_p$ (mm)	$4 \times 0.175$
	Volume (mm <sup>3</sup> )	122.808
Case 2	$H_p$ (mm)	10
	$W_p$ (mm)	Invariable=17.5
	$T_p$ (mm)	$4 \times 0.170$
	Volume (mm <sup>3</sup> )	119
Case 3	$H_p$ (mm)	16.9
	$W_p$ (mm)	10.187
	$T_p$ (mm)	Invariable= $4 \times 0.18$
	Volume (mm <sup>3</sup> )	123.955

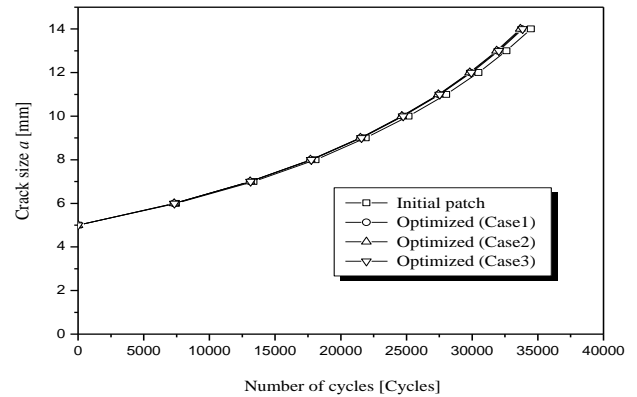


Fig. 10 Fatigue life predicted in the three optimized cases

Table 6 Optimized patch and fatigue life predicted in the three optimized cases

	Optimized patch	Number of cycles
Initial patch	252 mm <sup>3</sup>	34479
Case 1	122.808 mm <sup>3</sup>	33759
Case 2	119 mm <sup>3</sup>	33679
Case 3	123.955 mm <sup>3</sup>	33846

Once the patch is optimized, we can compare the fatigue life predicted by the considered three cases with the initial patch shape (Fig. 10).

It can be noticed that almost the same fatigue life is predicted for the three optimized cases (Table 6), comparatively to initial patch shape.

A small difference is estimated (800 cycles) between the number of cycles for optimized and non-optimized patch. Therefore, we can observe that optimization procedure is very useful, because it allows an important reduction of the patched volume for a very small decrease in fatigue life of the repaired.

### 5. Probability analysis of optimized patch

In the literature, optimization and reliability models are

rarely coupled (Errouane *et al.* 2014, Padula *et al.* 2006) to investigate the fatigue crack growth behaviour of repaired panels. Most of the authors develop the determinist models combined with the optimization procedure (Brighenti 2007, Youn *et al.* 2004). The probabilistic design process has not been widely used because it's high complexity. Used separately, these individual tools (optimization and reliability) require several manual iterations to attain the optimum design. In addition, optimum designs developed without consideration of uncertainty could possibly lead to unreliable designs. In addition to the active constraint problems, optimum designs may be sensitive to design parameters such that small changes in these parameters may lead to significant loss of performance (Khiat *et al.* 2011, Haldar and Mahadevan 2000). In this section, the modeling process for integrating the Probabilistic Design System (PDS) and the fatigue behavior modeling feature is developed in order to find the optimum design for the repaired aluminum panel (Fig. 1).

Reliability-based Optimization is a most appropriate and advantageous methodology for plate design. Its main feature is that it allows determining the best design solution while explicitly considering the unavoidable effects of uncertainty. The application of this methodology is numerically involved, as it implies the simultaneous solution of an optimization problem and also the use of specialized algorithms for quantifying the effects of uncertainties. Both, optimization and reliability assessment require the repeated evaluation of the structural response for different sets of design variables and uncertain parameters; in turn, the evaluation of the structural response may require the computation of numerically involved virtual simulation models.

The Monte Carlo Simulation (MCS) method is suitable for the present FEM because it allows handling a large number of design variables, when limit state function evaluations executed relatively quickly. This is the most common and traditional method for a probabilistic analysis. This method lets you simulate how virtual mechanical and geometrical parameters behave the way they are built. One simulation loop represents one manufactured parameters that is subjected to a particular set of loads and boundary conditions. When you manufacture a parameter, you can measure its geometry and all of its material properties. The method is always applicable regardless of the physical effect modeled in a finite element analysis. It not based on assumptions related to the random output parameters that if satisfied would speed things up and if violated would invalidate the results of the probabilistic analysis. Assuming the deterministic model is correct and a very large number of simulation loops are performed, then Monte Carlo techniques always provide correct probabilistic results. Of course, it is not feasible to run an infinite number of simulation loops; therefore, the only assumption here is that the limited number of simulation loops is statistically representative and sufficient for the probabilistic results that are evaluated.

The precision of the response depends on the number of evaluations and the chosen value of the failure probability. Uncertainties in numerical values are modeled as random input variables. In the present study, it was assumed that

Table 7 Random input variables of the model ( $a=14$  mm)

Input Parameters	Means	COV %	Standard deviation	Distribution
$W_p$ (mm)	17.5	5%	0.875	Lognormal
$H_p$ (mm)	20	5%	1	Lognormal
$T_p$ (mm)	0.72	9%	0.0648	Lognormal
$Ha$ (mm)	0.10	15%	0.015	Lognormal
$E_{11}$ (MPa.)	50 E3	12%	6000	Lognormal
$E_{22}$ (MPa.)	14.5 E3	12%	1740	Lognormal
$v_{12}$	0.33	5%	0.0165	Lognormal
$G_{12}$ (MPa)	2.56 E3	12%	307.2	Lognormal
$G_{23}$ (MPa)	2.24 E3	12%	268.8	Lognormal

Table 8 Mean values and standard deviations of the output parameters for initial and optimized patch shape

Case	$K_I$ (MPa $\sqrt{\text{mm}}$ )	Standard deviation
Without optimized patch	669.2	14.68
With optimized patch	662.2	16.17

geometrical and mechanical properties ( $E_{11}$ ,  $E_{22}$ ,  $v_{12}$ ,  $G_{12}$ ,  $G_{23}$ ,  $W_p$ ,  $H_p$ ,  $T_p$ ) of patch an adhesive layers ( $Ha$ ) are characterized by lognormal distributions (Table 7). This assumption is based on historical data (Khiat *et al.* 2011, Haldar and Mahadevan 2000). The mean value of the stress intensity factor is considered as a controllable parameter and it was declared as an optimization design variable (Table 8). The distribution parameters (mean values and standard deviations) are to defined for the random values in the model parameters.

The statistical post-processor provides the probability distribution functions of the output parameter, corresponding in our case to the stress intensity factor.

Both Figs. 12 and 13 represent the histogram of the stress intensity factor versus the relative frequency % before and after the patch optimization, respectively.

As shown in Fig. 12 and 13, the scatter of the histogram corresponding to the optimized patch is lower than for the initial patch. By considering the goodness-of-fit tests for the histograms in Fig. 13, it can be possible to identify the probability distribution model that fits better the MCS results. The lognormal distribution has been accepted by the statistical test, and can therefore be used to model the stress intensity factor.

Probability distribution of the output stress intensity factor simulated by the MCS method for initial and optimized patch shape is plotted in Fig. 14. Both curves are idealized by the lognormal distribution with large dispersion. It's shown that, the uncertainties of the optimized patch have the largest impact on the reliability of the model, because mechanical and geometrical properties are already optimized. Consequently, a small variation in manufacturing process of these properties can seriously affected the fatigue life of the repaired aluminum 2024 T3 plate.

Fig. 15 shows the cumulated probability functions (cpf) for initial and optimized patches. This pdf is therefore very useful to compute the fatigue life of the repaired aluminum 2024 T3 plates. At 50% of failure probability, the stress

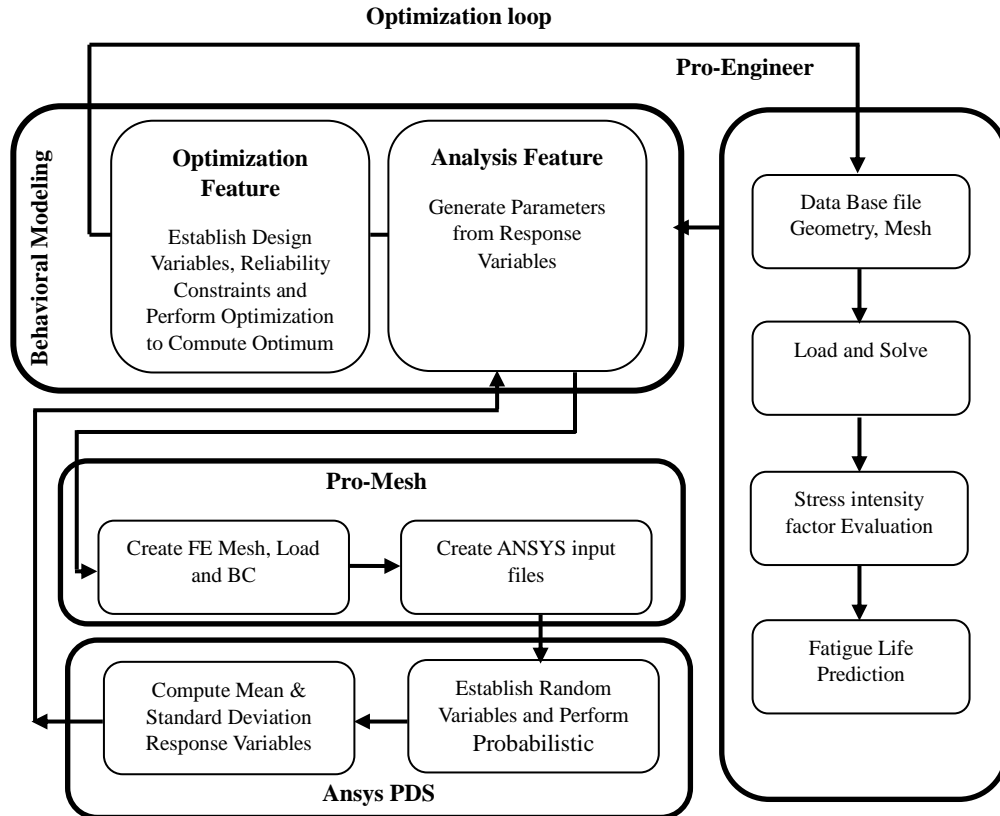


Fig. 11 Reliability based optimization fatigue crack of aluminum plate repaired using Pro/Engineers ANSYS

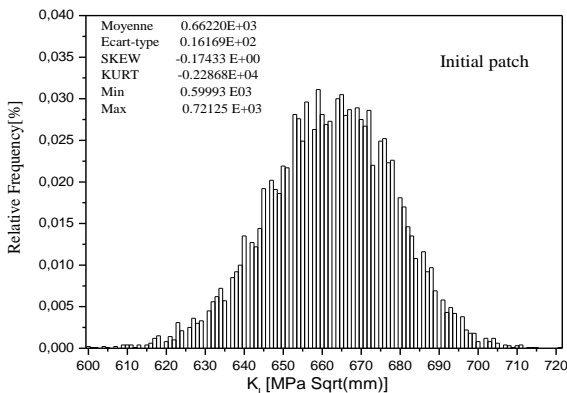


Fig. 12 Histogram of the stress intensity factor for Initial patch (Before Optimization)

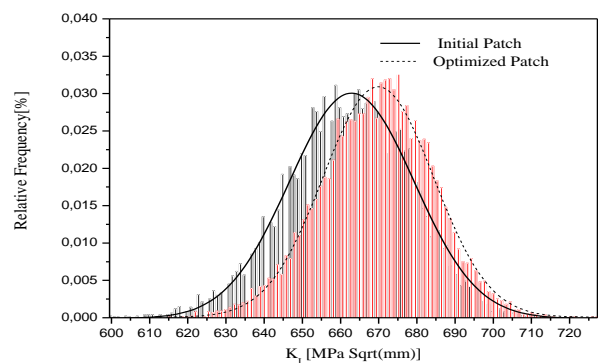


Fig. 14 Probability distributions of the stress intensity factor versus the relative frequency for the input random variables

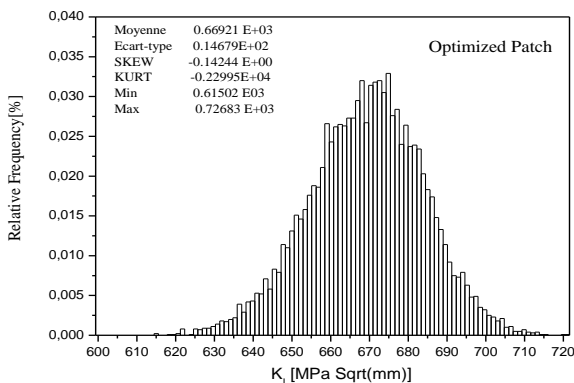


Fig. 13 Histogram of the stress intensity factor for Optimized patch (After Optimization)

intensity factor is  $661 \text{ MPa}\sqrt{\text{mm}}$  for initial patch and  $668 \text{ MPa}\sqrt{\text{mm}}$  for optimized patch; these values are close to the mean values as the probability distributions are almost symmetrical (i.e., low skewness). By selecting a target probability for the fatigue life assessment, the designer can specify the admissible stress intensity factor to be applied on the repaired plate. For example, if the admissible failure probability is set to  $10^{-4}$ , the corresponding stress intensity factor is  $602.1 \text{ MPa}\sqrt{\text{mm}}$  for initial patch and  $614.6 \text{ MPa}\sqrt{\text{mm}}$  for optimized patch. It can be confirmed that the probability of fatigue failure becomes larger for optimized patches. Consequently, the uncertainty study becomes more significant in the case of optimized structure.

Figs. 14 and 15 are both presented, because the probability density function is the probability (PDF) that the

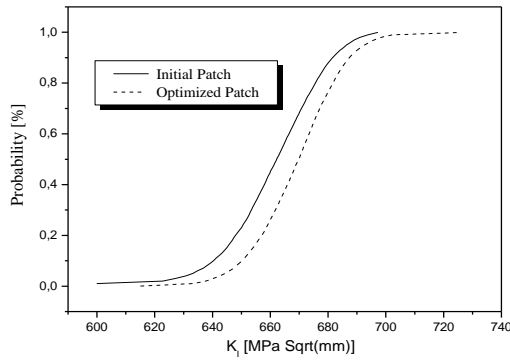


Fig. 15 Cumulative distribution curve of  $K_I$  with a reliability goal of 95%

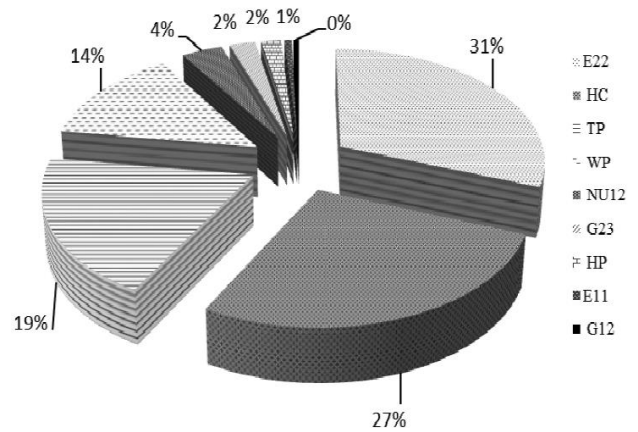


Fig. 17 Sensitivity analysis of  $K_I$  for random input variables for optimized patch

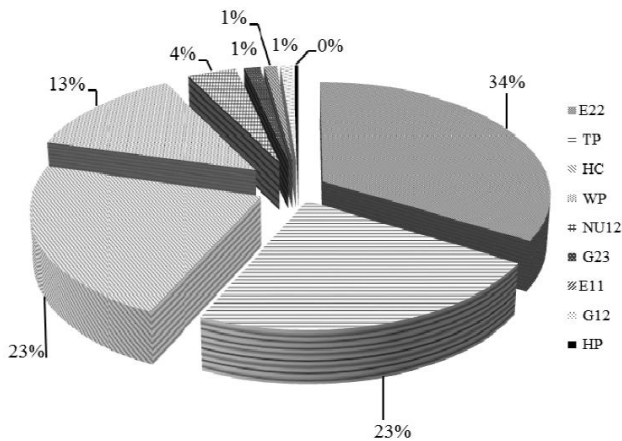


Fig. 16 Sensitivity analysis of  $K_I$  for random input variables for initial patch

stress intensity factor varies versus the relative frequency. If the PDF is largest, the model is probabilistic, contrary the model is determinist. But, the cumulative distribution function (CDF) used in the Fig. 15 is another method to describe the distribution of random variables (input parameters). The advantage of the CDF is that it can be defined for any kind of random variable (discrete, continuous or mixed).

Figs. 16 and 17 show the sensitivity of the stress intensity factor to random input variables for initial and optimized patch shapes. The sensitivity analysis of the input parameters regarding structural reliability depends on the statistical independency between input and output parameters.

The correlation coefficient chosen in this work is named the Spearman rank order correlation coefficient. In particular, a qualitative sensitivity measure of output parameter  $S_i$  with respect to input parameter  $R_i$  through the Spearman coefficient can be calculated

$$r_s = \frac{\sum_i^n (R_i - \bar{R})(S_i - \bar{S})}{\sqrt{\sum_i^n (R_i - \bar{R})^2} \sqrt{\sum_i^n (S_i - \bar{S})^2}} \quad (10)$$

where  $R_i$  is rank of input parameters within the set of observations  $[x_1, x_2, x_3, \dots, x_n]^T$

$S_i$  is rank of output parameters within the set of observations  $[y_1, y_2, y_3, \dots, y_n]^T$

$\bar{R}, \bar{S}$  are average ranks of the parameters  $R_i$  and  $S_i$  respectively.

The correlation coefficient measures a degree to which two variables are related (input and output parameters). The correlation coefficient takes values from -1.0 to 1.0, e.g., for  $r_s=1$  the input and output parameters are fully directly related, for  $r_s=0$  the input and output parameters are fully independent, while for  $r_s=-1$  the input and output parameters are fully inversely related. At this point it is necessary to specify that the correlation coefficient should be exclusively used when the variables satisfy the jointly normal distribution, input data is at least in the category of equal interval data and a relationship between variables is linear. If these requirements are not met, the non-parametric (distribution-free) measure by means of the Spearman correlation coefficient might be more appropriate.

In particular, the Spearman coefficient is more robust and it is the recommended one for cases where probabilistic information on the input variables is scarce. Its statistical test always gives an answer, e.g., in case when a relationship between variables is non-linear.

It can be seen that the transversal modulus ( $E_{22}$ ), thickness of adhesive layer ( $H_a$ ) and the thickness of patch ( $T_p$ ) are the important parameters, followed by ( $W_p$ ). These four variables are responsible of more than 93% of the effect on the fatigue life probability for initial patch, and the 91% for optimized patch, with the other five variables together making up for the remaining parts. Therefore, the four parameters should be paid more attention when designing the bonded patch repaired aluminum panels. They are followed by shear and Young's longitudinal modulus, Poisson's ratio and the height of the patch ( $H_p$ ) although the orders of sensitivity for some random input variables are different; they have no significant influence on the critical fatigue life, which can be ignored.

## 6. Conclusions

In the present paper, a probability analysis of optimal

design approach of fatigue non-uniform crack growth behavior of a cracked aluminum 2024 T3 plate repaired with a bonded composite patch was numerically investigated. The proposed model is implemented in finite element software and some numerical simulations were carried out in order to combine the optimization and reliability procedures to predict the best fatigue life. From the obtained results, it was noted that:

- Good agreement between the present model and results given in literature verifies the developed non-uniform crack growth procedure for patched and un-patched cracked aluminum plate.
- Reduction in stress intensity factor is one of the key issues in designing a patch. The relationship between the patch dimensions must be carefully selected in order to sufficiently cover the cracked zone, product a good reduction of stress intensity factor.
- Asymmetric repair of the cracked panels with bonded composite patch extended their fatigue lives by at least four times, and even in some cases much more.
- Crack growth is non-uniform across the repaired thickness of the panel. The difference between the crack lengths on the patched and un-patched faces was significantly bigger in thick panels than in thin panels.
- By adopting the optimal patch shape, the stress intensity factor can be reduced to about 50% with respect to that related to a square or rectangular shape patch.
- Optimization procedure is very useful, because an important reduction of the patched volume for a very small decrease in fatigue life of our repaired plate.
- Uncertainties of the optimized patch have the largest impact on reliability of our model. Consequently, a small variation in manufacturing process of these properties can seriously affected the fatigue life of the repaired aluminium 2024 T3 plate.
- Finally, the four input variables: transversal modulus, thickness of adhesive, the thickness of patch and with of the patch plate are responsible for the largest part of fatigue life reliability.

## References

- Baker, A.A., Rose L.R.F. and Jones, R. (2002), *Advances in the Bonded Composite Repairs of Metallic Aircraft Structures*, Vol. 1, Elsevier Science Publications, London.
- Brighenti, R. (2007), "Patch repair design optimization for fracture and fatigue improvements of cracked plates", *Int. J. Solid. Struct.*, **44**, 1115-1131.
- Denney, J.J. and Mall, S. (1997), "Characterization of disbond effects on fatigue crack growth behavior in aluminum plate with bonded composite patch", *Eng. Fract. Mech.*, **57**(5), 507-25.
- Errouane, H., Sereir, Z. and Chateauneuf, A. (2014), "Numerical model for optimal design of composite patch repair of cracked aluminium plates under tension", *Int. J. Adhes. Adhes.*, **49**, 64-72.
- Haldar, A. and Mahadevan, S. (2000), *Reliability Assessment Using Stochastic Finite Element Analysis*, John Wiley, New York, New York.
- Harman, A.B. and Rider, A.N. (2013), "On the fatigue durability of clad 7075-T6 aluminium alloy bonded joints representative of aircraft repair", *Int. J. Adhes. Adhes.*, **44**, 144-156.
- Hosseini-Toudeshky, H. and Mohammadi, B. (2009), "Mixed-mode numerical and experimental fatigue crack growth analyses of thick aluminium panels repaired with composite patches", *Compos. Struct.*, **91**, 1-8.
- Hosseini-Toudeshky, H., Mohammadi, B., Sadeghi, G. and Daghyani, H.R. (2007), "Numerical and experimental fatigue crack growth analysis in mode-I for repaired aluminum panels using composite material", *Compos. Part A-Appl. S.*, **38**, 1141-1148.
- Khiat, M.A., Sereir, Z. and Chateauneuf, A. (2011), "Uncertainties of unidirectional composite strength under tensile loading and variation of environmental condition", *Theor. Appl. Fract. Mech.*, **56**, 169-179.
- Lee, W.Y. and Lee, J.J. (2004), "Successive 3D FE analysis technique for characterization of fatigue crack growth behavior in composite-repaired aluminum plate", *Compos. Struct.*, **66**, 513-520.
- Mahadesh Kumar, A. and Hakeem, S.A. (2000), "Optimum design of symmetric composite patch repair to centre cracked metallic sheet", *Compos. Struct.*, **49**, 285-292.
- Murthy, A.R., Mathew, R.S., Palani, G.S., Gopinath, S. and Iyer, N.R. (2015), "Fracture analysis and remaining life prediction of aluminium alloy 2014a plate panels with concentric stiffeners under fatigue loading", *Struct. Eng. Mech.*, **53**(4), 681-702.
- Padula, S., Gumbert, C. and Li, W. (2006), "Aerospace Applications of Optimization under Uncertainty", *Optim. Eng.*, **7**(3), 317-328.
- Paris, P.C. and Erdogan, F. (1963), "Critical analysis of crack propagation laws", *Tran. ASME Ser. D: J. Basic Eng.*, **85**, 528-534.
- Sekine, H., Yan, B. and Yasuho, T. (2005), "Numerical simulation study of fatigue crack growth behavior of cracked aluminum panels repaired with a FRP composite patch using combined BEM/FEM", *Eng. Fract. Mech.*, **72**, 2549-2563.
- Seo, D.C., Lee, J.J. (2002), "Fatigue crack growth behavior of cracked aluminum plate repaired with composite patch", *Compos. Struct.*, **57**, 323-330.
- Tsai, G.C. and Shen, S.B. (2004), "Fatigue analysis of cracked thick aluminium plate bonded with composite patches", *Compos. Struct.*, **64**, 79-90.
- Wang, X., Shi, J., Liu, J., Yang L., Wu, Z. (2014), "Creep behavior of basalt fiber reinforced polymer tendons for prestressing application", *Mater. Des.*, **59**, 558-564.
- Yan, Y. (2004), "Design of structure optimization with APDL", *J. East China Jiaotong Univ.*, **4**, 52-55.
- Youn, B.D., Choi, R.J. and Gu, L. (2004), "Reliability-based design optimization for crash worthiness of vehicle side impact", *Struct. Multidisc. Optim.*, **26**, 272-283.